Removal of ortho-phosphate from aqueous solution by adsorption onto dolomite

Chirangano Mangwandi[1]*, Ahmad B. Albadarin[1], Yoann Glocheux[1], Gavin M. Walker[1, 2]

[1]School of Chemistry and Chemical Engineering, Queen's University Belfast,
Belfast BT9 5AG, Northern Ireland, UK.

[2]Materials Surface Science Institute,
Department of Chemical and Environmental Sciences,
University of Limerick,
Ireland.

*Corresponding Author
Dr Chirangano Mangwandi
Tel: +44 (0) 28 9097 4378
Fax: +44 (0) 28 9097 6524
E-mail: c.mangwandi@qub.ac.uk

Abstract

An experimental study on the adsorption of phosphate onto cost effective fine dolomite powder is presented. The effect of solution pH, solution ionic strength and adsorption isotherm were examined. The adsorption of phosphate was pH dependent and phosphate adsorption favoured acidic conditions, with a maximum uptake of 377. mg g^{-1} at pH 2. The adsorption was significantly influenced by solution ionic strength indicating outer-sphere complexation reactions. The experimental data further indicated that the removal of phosphate increased with increase in the ionic strength of solution. The experimental data was modelled with different isotherms, such as: Langmuir, Freundlich and Redlich–Peterson isotherms; on analysis it was found that the Redlich–Peterson isotherm depicted the equilibrium data accurately. The overall kinetic data fitted very well the pseudo first-order rate model.

1. Introduction

Phosphate is one of the most important nutrients essential for plant growth and modern agricultural methods [1]. Phosphate is discharged to water by various human activities; industrial and agricultural applications. The extensive discharge of phosphate into surface water can cause eutrophication, and thus lower the water quality [2]. Therefore, effective phosphate recovery techniques will prevent the pollution of water environment and overcome the resource deficiency issue. The removal technologies for aqueous phosphate or phosphorous from contaminated waters include: crystallization, chemical precipitation and biological removal. In phosphate removal investigations regarding crystallization [3-5], a number of materials such as sand and Ca-phosphate crystals were utilized as seeding materials to initiate and improve phosphate recycling and precipitation. However, a crystallization method requires complicated and precise control of the operating conditions [1, 6]. Chemical precipitation and biological removal have other disadvantages such as: the cost of chemicals, substantial additional sludge production and phosphorus release in the sludge treatment [7].

Adsorption is becoming an increasingly important process for the elimination of contaminants from waste waters [8, 9]. A detailed review of P nutrient removal and recovery technologies was given by Morse [10]. The adsorption technique offers a number of advantages over the other techniques for instance it allows use of low cost materials for remediation of contaminated waste water; the process scale-up is easy and low operational costs [11]. Several studies on the removal of phosphorus/ phosphate from contaminate waters using the adsorption method have been given in literature [12-17]. Dolomite [$CaMg(CO_3)_2$], a material that is existing abundantly and cheaply worldwide [18] is the subject of attention for more than six decades [11]. Despite a relatively low specific surface area (~1.50 $m^2 g^{-1}$) [19], dolomite still shows some good adsorption properties. Karaca et al. carried out a comparison between calcinated dolomite and raw dolomite in terms of capacity of phosphate removal from aqueous

solution [20]. Authors reported that the phosphate capacity increased with an increased in the solution pH at a solid-liquid ratio 2.0 g/L, adsorption temperature 20 ºC and ionic strength 0.0 M. Authors reported that the Phosphate removal decreased with increasing temperature and slightly increased with increasing of pH. It was suggested that the main mechanisms for adsorption of phosphate on dolomite could be both physical interactions and chemi-sorption.

This research was carried out to investigate the removal of phosphate from aqueous solutions by adsorption onto low cost dolomite materials, through equilibrium and kinetic studies. This research differs from the earlier studies [20, 21] in a number of ways. Firstly, higher initial concentrations of phosphate solution were used to match the typical phosphate levels in slurries from anaerobic digestion plants. Unlike in the previous research reports, where coarse particle of adsorbent were used, this research used very fine raw dolomites powder as this size allows further processing of the powder after adsorption for use as soil-conditioner [22-24]. Secondly, this paper studies the effect of solution ionic strength which has not been studied before. Further insights on the mechanism and nature of the adsorption process were gained by applying appropriate equilibrium and kinetic models to the experimental data.

2. Materials and Methods

2.1 Chemicals

Calcium phosphate monobasic manufactured and supplied by Aldrich – Chemical Co. Ltd, UK was used as the source of phosphate ions. The adsorbent used in this research was fine dolomite supplied by Kilwaughter Chemical Company, UK, which had a particle size between 50–100 µm. The fine dolomite in this study has been tested for adsorption experiments without any pre-treatment. Solutions of 1M of HCl and NaOH were used for the manual control of pH (pH meter, Thermo Fisher scientific-Singapore). The electrolyte used to modify the ionic strength in the adsorption experiments was NaCl.

2.2 Equipment

A XRD analysis was performed to examine the crystalline nature of the fine dolomite sample (Wide angle X-ray diffraction using a Philips panalytical X'pert pro diffractometer). The surface structure of the fine dolomite was explored with Fourier Transform Infrared Spectroscopy (FT-IR), to illustrate the change in the functional groups of the dolomite surface before and after adsorption. The structural ordering of the fine dolomite was analyzed by scanning electron microscopic (SEM), using a JEOL-JSM 6400 scanning microscope. For batch equilibrium studies, samples have been regularly shaken (mechanical shaker, GerhardT type LS 5) for 7 days at 100 rpm and 20 °C. The initial and final concentrations of the nutrients were measured by inductive couple plasma (ICP-OES, Optima 4300 DV, 16 Perkin Elmer, USA). The surface area and the cumulative pore size distribution of the dolomite powder were measured using a mercury porosimetry (PoreMaster®, QuantaChrome Instruments).

2.3 Adsorption Experiment

The influence of solution pH on adsorption capacity was investigated by adding 0.2 g of adsorbent to 250 mL bottle jars containing 50 mL solutions solution (C_o =1000 mg P/L) at room temperature (20 ºC). The experiment was performed using solutions at various pH values: 2 to 10. The influence of ionic strength on the adsorption of phosphate onto dolomite was examined by altering the initial phosphate concentrations 100 and 2000 mg/L in the existence of NaCl salt, at three altered concentrations 0.05, 0.1 and 0.3 M. This value was selected based on the average ionic strength values used in phosphate adsorption research paper reported in literature [25, 26]. Batch equilibrium studies were performed by adding 0.2 g of adsorbent to 250 mL bottle jars containing 50 mL solutions of altered initial concentrations (100–2000 mg P/L) and agitated at 100 rpm using mechanical shaker, GerhardT type. The equilibrium time for all experiments was 7 days. After the adsorption equilibrium was achieved, solutions were filtered to remove the fine dolomite, transferred into polythene tubes and diluted prior to

125 analysis. The amount of phosphate adsorbed at equilibrium, q (mg/g), which corresponds to
126 the difference in phosphate concentration in the solution before and after adsorption was
127 calculated using the following equation:

$$q = \frac{V(C_o - C_e)}{m_s} \quad \textbf{(1)}$$

128 where C_o and C_e (mg P/L) are the concentration of nutrient at initial and equilibrium,
129 correspondingly, V is the volume of the solution (L) and m_s is the mass of dolomite (g).

130 For kinetic studies, 1.0 g of the adsorbent material was contacted with 250 mL of phosphate
131 solution with initial concentration 1000 mg P/L and stirred by a magnetic stirrer. Samples were
132 taken at ordinary time intervals. The solution pH was not adjusted for this set of experiments;
133 the solution had an initial pH 4. However, 100 mg.L^{-1} of $NaHCO_3$ was added in solutions used
134 in adsorption experiments as a pH buffer. The phosphate uptake at any time q_t (mg/g) was
135 calculated using Eq. (1). To compare the capability of each adsorption isotherm and kinetic
136 model to predict the experimental data, a standard deviation is calculated as follows [27-30];

$$SD = \sqrt{\frac{\sum\left(\left(q_{t,\exp} - q_{t,\mathrm{mod}}\right)/\, q_{t,\exp}\right)^2}{N-1}} \quad \textbf{(2)}$$

137 where N is the number of data points, $q_{t,\exp}$ and $q_{t,\mathrm{mod}}$ are the measured and calculated
138 concentrations of adsorbate in solid phase respectively.
139

140 ## 3. Results and Discussion

141 ### 3.1 Characterization of Adsorbent

142 The performance of an adsorption material is influenced by the porosity and surface area
143 available for adsorption. Fig. 1 shows the cumulative pore size distribution of the dolomite

144 powder. It was found that the powder median pore-diameter, $d_{50,}$ of 15 µm. This means that
145 pores of size of about 15 µm or less contribute to about 50% of the pore surface area; the
146 adsorbent can therefore be described as being macroporous. The surface area of the dolomite
147 was 0.146 m^2/g measured by the mercury porosimetry. Semi-quantitative analysis of the data
148 given in Table 1 indicates that the main component is calcite which is about 68%. The
149 comparison between the XRD profiles before and after adsorption with phosphate is shown in
150 Fig. 2. The X-Ray Diffraction analysis undertaken on the dolomite powder presented in Fig.
151 2a illustrates that the main components are calcite, dolomite, quartz and periclass. It can be
152 noted from Fig. 2b that adsorption of phosphate has the effect of shifting the peaks to the left.
153 There is also a significant reduction in the main calcite peaks which suggests that there may be
154 some dissolution of carbonate during the experiment. The phosphate adsorption onto dolomite
155 results in the appearance of a sharp new peak at around 2θ of 11º and an increase in the
156 intensity of the peak ~ 21º (see Fig. 2b). This phenomena indicate the formation of $Mg_3(PO_4)_2$
157 and $Ca_3(PO_4)_2$ and the crystalline nature of these precipitates [31].

158 FTIR analysis undertaken on the dolomite before and after adsorption of phosphate is
159 presented in Fig. 3. A broad and intense band of O–H stretching vibration around 3500–3300
160 cm^{-1} and a band around 1700 cm^{-1} (O–H bending vibration) specified the existence of
161 coordinated water molecule [32]. The existence of silicate phases (Si–O vibrations) can be seen
162 at 1040 cm^{-1} and the band at 1437.1 cm^{-1} may be assigned to CO_3^{2-} group [11]. There is a
163 noticeable increase in the intensity of –OH group, which can be attributed to the attraction
164 between the protonated –OH groups and phosphate ions i.e., electrostatic attraction. The
165 reduction of CO_3^{2-} group band may indicate the substitution of carbonates on the dolomite by
166 phosphate ions. There is also a corresponding increase in the bands associated with phosphate
167 group at frequencies of 471, 566, 604 and 961cm^{-1}. The new band at 1050 cm^{-1} can be due to
168 the bending vibration of adsorbed phosphate [33]. The FT-IR spectra showed that calcium

phosphate precipitates were formed and phosphate fixation with Mg^{2+} in amorphous form can be predicted. The fine dolomite surface topography before and after phosphate adsorption was examined by SEM, and the results are revealed in Fig.4. In fresh dolomite particles (Fig. 4a), the particles are covered with amorphous fuzzy materials, whereas the surface of the loaded fine dolomite is almost crystalline. The presence of fines at the surface of the samples underlines the very brittle nature of the materials used in the study. The crystalline structure reveals the formation of $Ca_3(PO_4)_2$ and/or $Mg_3(PO_4)_2$ through surface precipitation [34].

3.2 Effect of solution pH

The effect of altering the pH of the solution on the adsorption of phosphate ions onto dolomite adsorbent after 7 days is shown in Fig. 5. The adsorption capacity decreased considerably with increasing of solution pH form 2 to 10. This clearly shows that the adsorption of phosphate ions onto fine dolomite is pH dependent and that the phosphate adsorption favoured acidic conditions, with a maximum uptake of 227.3 mg P/g at pH 2. $H_2PO_4^-$ and HPO_4^{2-} are dominant phosphate species in the solution under the tested pH range [35]. At low pH (i.e. pH < 4), the adsorbent surface is the positively charged and favours the adsorption of phosphate ions. The point of zero charge (PCZ) of dolomite was previously determined as 8.55 [11]. Similar trends have been found by other several studies showing dependence of sorption of phosphate on pH of the solution [15, 16, 36].

On the other hand, increasing the pH decreased the uptake of phosphate on fine dolomite. It is known that the adsorption of oxyanion onto negatively charged adsorbent surface sites is not favoured due to the electrostatic repulsion [37]. The reduction in the capacity of adsorption with an increase in pH is attributed to competition for the positively charged sites on the adsorbent as high pH. As the pH of the solution increases the OH^- species in the solution increases, these compete for positive sites on the adsorbent surface with the target PO_4^{3-} ions and the amount of adsorption is consequently dropped. Dolomite is mainly

194 composed of $MgCO_3$ and $CaCO_3$. Dolomite surface is rough, which perhaps results in
195 chemisorption of phosphate ions attributed to increasing the possibility of solid contact. In
196 addition, at low pH values, this could increase the adsorption of phosphate onto dolomite in
197 the form of $Mg_3(PO_4)_2$ and $Ca_3(PO_4)_2$ [11, 21]. Surface precipitation of P with Ca to form
198 corresponding phosphates of discrete solid phase, is a possible mechanism for phosphate
199 removal onto fine dolomite [38].

200 **3.3 Effect of Ionic Strength**

201 Fig. 6 shows the effect of ionic strength on the removal of phosphate ions by fine
202 dolomite at two different initial phosphate concentrations (100 and 2000 mg/L). It was found
203 that as the ionic strength increased from 0.05 to 0.3 M, the adsorption of phosphate increased
204 from 58.3 to 81.4 mg P/g and form 371.0 to 583.1 mg P/g for phosphate initial concentrations
205 100 and 2000 mg P/L, respectively. The ionic strength dependence indicates an outer-sphere
206 complexation reactions [39]. Similar results have been described by Zhang et al. (2009) [35]
207 for phosphate adsorption from water by a Fe–Mn binary oxide adsorbent.

208 The Na ions may enhance the adsorption of phosphate by reducing the repulsion
209 between the phosphate ions adsorbed on the surface. It can also be observed from Fig. 6 that
210 for high initial concentration of P, increasing the ionic strength from 0.05 M to 0.1 M results
211 in an increase in the q_e (almost doubles) though a further increase to 0.3 M results in a slight
212 reduction in the q_e value. This may be due to the high concentration of Cl^- ions which will act
213 as competitive ions for the adsorption sites. Antelo et al. (2005) [40] indicated that the salt
214 effect was stronger and the adsorption increased by increasing NaCl concentration at solution
215 pH 6. The increase in phosphate uptake with increase of NaCl concentration maybe also due
216 to the macromolecular phosphate configuration [41]. The negatively charged phosphate
217 macromolecules are screened and therefore the phosphate molecules wounded up like

unsystematic coils. In this more compressed arrangement, more phosphate can be sorbed onto a given area of adsorbent surface.

3.4 Equilibrium modelling

3.4.1. Freundlich Isotherm

The Freundlich isotherm explains a particular phenomena when the adsorption takes place on a heterogeneous surface [42]. The Freundlich isotherm model is given in Eq. 3:

$$q_e = K_F C_e^{1/n} \quad \textbf{(3)}$$

where K_F and n are the Freundlich constants. The Freundlich isotherm constants obtained from non-linear regression fitting are revealed in Table 2.

3.4.2. Langmuir Isotherm

The Langmuir isotherm described an adsorption process taking place at specific homogenous sites with a uniform distribution of energy within the adsorbent surface.

The Langmuir isotherm is given in Eq. 4:

$$q_e = q_{\max}\left[\frac{bC_e}{1+bC_e}\right] \quad \textbf{(4)}$$

where Langmuir constant a_L (L/mg) is corresponds to the adsorption energy and $K_L = q_{max} \times a_L$; q_{max} is the Langmuir monolayer capacity.

The Langmuir constants can be employed to calculate, R_L, the separation factor which is given by:

$$R_L = \frac{1}{1+(K_L)C_o} \quad \textbf{(5)}$$

A value of R_L between 0 and 1 indicates adsorption is favourable, while $R_L > 1$ indicates an unfavourable adsorption process [43].

3.4.3. Redlich & Peterson Isotherm

Redlich and Peterson isotherm which can explain the adsorption process over a wide range of concentrations integrates some features of both the Langmuir and Freundlich isotherms as given in Eq. 6:

$$q_e = \frac{K_R C_e}{1 + a_R C_e^{\beta}} \quad \textbf{(6)}$$

where a_R (L/mg) and β are the isotherm constants and K_R is the modified Langmuir constant (L/g). Commercial software (SigmaPlot version 11.0, Systat Software Inc.) was used to perform non-linear regression fits of isotherm equations.

To confirm the previous findings, the influence of ionic strength on the adsorption of phosphate onto fine dolomite was also studied at six different concentrations in order to obtain adsorption equilibrium isotherms after 7 days contact time. Langmuir, Freundlich and Redlich–Peterson models were employed to describe the experimental data and results are revealed in Table 2 and Fig. 7 (For 0.0 M NaCl only). It is apparent from Table 2 and Fig. 7 that Redlich–Peterson isotherm provides the best fit to the experimental data at all NaCl concentrations studied with R^2 values higher than 0.957. Also, apart from at 0 M NaCl concentration, the values of standard deviation for Redlich–Peterson isotherm were lower than those for Frendlich and Langmuir isotherms at all experimental conditions studied. However, the Freundlich isotherm constant, *n*, which is an indication of adsorption intensity was higher than unity suggesting that the adsorption of phosphate onto fine dolomite is favourable [44]. The separation factor, R_L, values for the adsorption of phosphate onto dolomite were in the range of 0.088–0.173 (Table 2) which indicates that the adsorption is a favourable process.

3.5. Adsorption Kinetics

The pseudo-first-order and pseudo-second-order kinetic models were fitted to the kinetic data. The intra-particle diffusion and Elovich models were also employed to find out the adsorption diffusion mechanisms. The SD values for the different models are given in Table 3.

The adsorption kinetics may be explained by pseudo first order model [11];

$$q_t = q_e\left(1 - e^{-k_1 t}\right) \quad \textbf{(7)}$$

This can also be given in a linear form as;

$$\ln\left(q_e - q_t\right) = \ln\left(q_e\right) - k_1 t \quad \textbf{(8)}$$

where k_1 is the rate constant for first order adsorption (min^{-1}). The linear plot of $\ln\left(q_e - q_t\right)$ versus t is shown in Fig. **8** (a).

The kinetic data for adsorption can also be explained by the pseudo-second-order equation which is expressed as;

$$q_t = \frac{q_e^2 k_2 t}{1 + q_e k_2 t} \quad \textbf{(9)}$$

The linear form of the pseudo second order equation can be given as;

$$\frac{t}{q_t} = \frac{1}{k_2 q_e^2} + \frac{1}{q_e} t \quad \textbf{(10)}$$

where k_2 (g/mg h) is the adsorption rate constant for the second-order model. q_e is the equilibrium adsorption capacity and k_2 (g/mg h) calculated from the slope and intercept of plot t/q_t versus t (Fig. **8** (b)). The constants k_2 and q_e determined from the model are shown in Table 3 along with the corresponding correlation coefficients.

The intra-particle diffusion model can be given as [45]:

$$q_t = K_{di} t^{1/2} + C_i \quad \textbf{(11)}$$

where K_{di} is the rate constant for intra-particle diffusion model (mg $g^{-1}h^{-1/2}$) and the intercept, C_i corresponds to the thickness of the adsorption layer (Fig. 8(c)). Intra-particle diffusion is controlled by the diffusion of ions within the pores of the adsorbent [46].

Elovich equation is one of the most practical models for predicting chemisorption processes, which can be expressed as [43, 47]:

$$q_t = \frac{1}{b}\ln(ab) + \frac{1}{b}\ln t \quad \textbf{(12)}$$

where a (mg g^{-1}) is the initial sorption rate and b (mg $g^{-1}h^{-1}$) is related to the extent of surface coverage and activation energy for chemisorptions. The plot of the Elovich model is shown in Fig. 8 (d). The $1/b$ value indicates the number of sites available for adsorption whereas the term $1/b \ln(ab)$ is the adsorption magnitude when $\ln t$ is equal to zero; i.e., the adsorption quantity when t is 1 h [48]. This value is useful in realizing initial adsorption behaviour [49]. Non-linear regression was carried out on the kinetic data using equations 7, 9, 11, and 12. The model parameters obtained from non-linear regression are given in Table 3. Values of determination coefficient, R^2, for both the pseudo-first and second-order models are > 0.990, suggesting that the models give a good fit. Similar trends were obtained for the Cr(VI) adsorption by dolomite [11]. It was declared that the pseudo kinetic models are empirical equations that do not give a precise understanding of the physio-chemical processes which are occurring.

However, the pseudo-first-order has the least SD value which implies that it provides a better demonstration of the experimental data. On the other hand, for the pseudo-second-order, it can be noted from Fig. 8 (b) that a better fit can be obtained by dividing the data into two sections which can be representative of different modes of adsorption occurring on the dolomite powder. Fig. 8 (c) also illustrates that the adsorption plots were not linear over the entire time

range and can be divided into two linear regions which validate that the adsorption is a multi-stages process. The initial segment is regarded as a physisorption (i.e. ion exchange or surface precipitation) and the second segment is attributed to the intra-particle diffusion effects [39]. Furthermore, the plots are linear in the initial stage of adsorption and the linearized data did not pass through the origin signifying that intra-particle diffusion was not only the rate-limiting step [37]. The Elovich equation also gave an acceptable fitting to the experimental data and followed the pseudo second-order process. The Elovich model is suitable for systems with heterogeneous adsorbing surfaces and suggests chemical adsorption processes with the adsorption rate decreasing with time due to an increase in surface coverage [50].

3.6. Comparison of adsorption capacity with various adsorbents

The adsorption capacity of the fine dolomite determined in this study was compared with that of other adsorbents adsorption capacities reported in the literature is shown in Table 4. Dolomite material showed a higher adsorption capacity of phosphate than those of the reported adsorbents. This may be attributed to the high initial phosphate concentration used, the individual adsorbent characteristics and it ability to remove phosphate ions via precipitation and ion exchange mechanisms [11]. It also suggests that dolomite is more applicable than the other adsorbents for wastewater with a high phosphate concentration.

4. Conclusion

Fine dolomite was examined for the adsorption of phosphate from aqueous solutions. The removal of phosphate from aqueous solutions was found to be significantly dependent on the pH of the solution and ionic strength. The maximum adsorption capacity was achieved at pH 2. The monolayer adsorption capacity calculated form the Langmuir isotherm was obtained 227.3 mg Pg^{-1} (optimum pH 2.0, ionic strength 0.0 M NaCl, 0.80 g L^{-1} adsorbent mass,

317 temperature (20 ◦C) and 7 days contact time). The equilibrium isotherm data was accurately
318 described by the Redlich–Peterson isotherm model. The results show that fine dolomite is an
319 effective adsorbent for the removal and recovery of phosphate ions from aqueous solutions
320 under the tested experimental conditions.
321

5. Reference

[1] T. Ogata, S. Morisada, Y. Oinuma, Y. Seida, Y. Nakano, Preparation of adsorbent for phosphate recovery from aqueous solutions based on condensed tannin gel, Journal of Hazardous Materials, 192 (2011) 698-703.

[2] C. Mangwandi, A.B. Albadarin, G.M. Walker, S.J. Allen, Nutrient recovery form waste water: optimization of adsorption process, Chemical Engineering Transactions, 24 (2011) 1177-1182.

[3] N. KarapInar, Application of natural zeolite for phosphorus and ammonium removal from aqueous solutions, Journal of Hazardous Materials, 170 (2009) 1186-1191.

[4] N. Karapinar, E. Hoffmann, H.H. Hahn, P-recovery by secondary nucleation and growth of calcium phosphates on magnetite mineral, Water Research, 40 (2006) 1210-1216.

[5] A. Ugurlu, B. Salman, Phosphorus removal by fly ash, Environment International, 24 (1998) 911-918.

[6] K. Suzuki, Y. Tanaka, T. Osada, M. Waki, Removal of phosphate, magnesium and calcium from swine wastewater through crystallization enhanced by aeration, Water Research, 36 (2002) 2991-2998.

[7] P.M.J. Janssen, K. Meinema, R.H. F., Biological Phosphorus Removal: Manual for Design and Operation, IWA Publishing, (2002) 11-13.

[8] A.B. Albadarin, C. Mangwandi, A.H. Al-Muhtaseb, G.M. Walker, S.J. Allen, M.N.M. Ahmad, Modelling and Fixed Bed Column Adsorption of Cr(VI) onto Orthophosphoric Acid-activated Lignin, Chinese Journal of Chemical Engineering, 20 (2012) 469-477.

[9] Y.A. Ouaissa, M. Chabani, A. Amrane, A. Bensmaili, Removal of tetracycline by electrocoagulation: Kinetic and isotherm modeling through adsorption, Journal of Environmental Chemical Engineering, 2 (2014) 177-184.

[10] G.K. Morse, S.W. Brett, J.A. Guy, J.N. Lester, Review: Phosphorus removal and recovery technologies, The Science of The Total Environment, 212 (1998) 69-81.

[11] A.B. Albadarin, C. Mangwandi, A.a.H. Al-Muhtaseb, G.M. Walker, S.J. Allen, M.N.M. Ahmad, Kinetic and thermodynamics of chromium ions adsorption onto low-cost dolomite adsorbent, Chemical Engineering Journal, 179 (2012) 193-202.

[12] M.F. Abou Taleb, G.A. Mahmoud, S.M. Elsigeny, E.-S.A. Hegazy, Adsorption and desorption of phosphate and nitrate ions using quaternary (polypropylene-g-N,N-dimethylamino ethylmethacrylate) graft copolymer, Journal of Hazardous Materials, 159 (2008) 372-379.

[13] N.M. Agyei, C.A. Strydom, J.H. Potgieter, An investigation of phosphate ion adsorption from aqueous solution by fly ash and slag, Cement and Concrete Research, 30 (2000) 823-826.

[14] M.Y. Can, E. Yildiz, Phosphate removal from water by fly ash: Factorial experimental design, Journal of Hazardous Materials, 135 (2006) 165-170.

[15] M. Özacar, Phosphate adsorption characteristics of alunite to be used as a cement additive, Cement and Concrete Research, 33 (2003) 1583-1587.

[16] L. Ruixia, G. Jinlong, T. Hongxiao, Adsorption of Fluoride, Phosphate, and Arsenate Ions on a New Type of Ion Exchange Fiber, Journal of Colloid and Interface Science, 248 (2002) 268-274.

[17] A. Drizo, C.A. Frost, J. Grace, K.A. Smith, Physico-chemical screening of phosphate-removing substrates for use in constructed wetland systems, Water Research, 33 (1999) 3595-3602.

[18] E. Pehlivan, A.M. Özkan, S. Dinç, Ş. Parlayici, Adsorption of Cu2+ and Pb2+ ion on dolomite powder, Journal of Hazardous Materials, 167 (2009) 1044-1049.

[19] A. Duffy, G.M. Walker, S.J. Allen, Investigations on the adsorption of acidic gases using activated dolomite, Chemical Engineering Journal, 117 (2006) 239-244.
[20] S. Karaca, A. Gürses, M. Ejder, M. AçIkyIldIz, Adsorptive removal of phosphate from aqueous solutions using raw and calcinated dolomite, Journal of Hazardous Materials, 128 (2006) 273-279.
[21] S. Karaca, A. Gürses, M. Ejder, M. AçIkyIldIz, Kinetic modeling of liquid-phase adsorption of phosphate on dolomite, Journal of Colloid and Interface Science, 277 (2004) 257-263.
[22] C. Mangwandi, A.B. Albadarin, L. JiangTao, S. Allen, G.M. Walker, Development of a value-added soil conditioner from high shear co-granulation of organic waste and limestone powder, Powder Technology, 252 (2014) 33-41.
[23] C. Mangwandi, L. JiangTao, A.B. Albadarin, S.J. Allen, G.M. Walker, Alternative method for producing organic fertiliser from anaerobic digestion liquor and limestone powder: High Shear wet granulation, Powder Technology, 233 (2013) 245-254.
[24] A.B. Albadarin, C. Mangwandi, G.M. Walker, S.J. Allen, M.N.M. Ahmad, M. Khraisheh, Influence of solution chemistry on Cr(VI) reduction and complexation onto date-pits/tea-waste biomaterials, Journal of Environmental Management, 114 (2013) 190-201.
[25] Jianyong Liu, Lihua Wan, Ling Zhang, Q. Zhou, Effect of pH, ionic strength, and temperature on the phosphate adsorption onto lanthanum-doped activated carbon fiber, Journal of Colloid and Interface Science, 364 490–496.
[26] Renkou XU, Yong WANG, Diwakar TIWARI, H. WANG, Effect of ionic strength on adsorption of As(III) and As(V) on variable charge soils Original Research Article, Journal of Environmental Sciences, 21 (2009) 927-932.
[27] B.H. Hameed, A.A. Rahman, Removal of phenol from aqueous solutions by adsorption onto activated carbon prepared from biomass material, Journal of Hazardous Materials, 160 (2008) 576-581.
[28] L. Johansson, J.P. Gustafsson, Phosphate removal using blast furnace slags and opoka-mechanisms, Water Research, 34 (2000) 259-265.
[29] M. Özacar, Contact time optimization of two-stage batch adsorber design using second-order kinetic model for the adsorption of phosphate onto alunite, Journal of Hazardous Materials, 137 (2006) 218-225.
[30] F.-C. Wu, R.-L. Tseng, R.-S. Juang, Kinetic modeling of liquid-phase adsorption of reactive dyes and metal ions on chitosan, Water Research, 35 (2001) 613-618.
[31] S. Liodakis, G. Katsigiannis, T. Lymperopoulou, Ash properties of Pinus halepensis needles treated with diammonium phosphate, Thermochimica Acta, 453 (2007) 136–146.
[32] L.A. Rodrigues, M.L.C.P. da Silva, Thermodynamic and kinetic investigations of phosphate adsorption onto hydrous niobium oxide prepared by homogeneous solution method, Desalination, 263 (2010) 29-35.
[33] H. Liu, X. Sun, C. Yin, C. Hu, Removal of phosphate by mesoporous ZrO_2, Journal of Hazardous Materials, 151 (2008) 616-622.
[34] S. Moharami, M. Jalali, Removal of phosphorus from aqueous solution by Iranian natural adsorbents, Chemical Engineering Journal, 223 (2013) 328-339.
[35] G. Zhang, H. Liu, R. Liu, J. Qu, Removal of phosphate from water by a Fe-Mn binary oxide adsorbent, Journal of Colloid and Interface Science, 335 (2009) 168-174.
[36] S. Tanada, M. Kabayama, N. Kawasaki, T. Sakiyama, T. Nakamura, M. Araki, T. Tamura, Removal of phosphate by aluminum oxide hydroxide, Journal of Colloid and Interface Science, 257 (2003) 135-140.
[37] T. Tuutijärvi, E. Repo, R. Vahala, M. Sillanpää, G. Chen, Effect of Competing Anions on Arsenate Adsorption onto Maghemite Nanoparticles, Chinese Journal of Chemical Engineering, 20 (2012) 505-514.

[38] J.B. Xiong, Q. Mahmood, Adsorptive removal of phosphate from aqueous media by peat, Desalination, 259 (2010) 59-64.
[39] L.E. Katz, L.J. Criscenti, C.-C. Chen, J.P. Larentzos, H.M. Liljestrand, Temperature effects on alkaline earth metal ions adsorption on gibbsite: Approaches from macroscopic sorption experiments and molecular dynamics simulations, Journal of Colloid and Interface Science, 399 (2013) 68-76.
[40] J. Antelo, M. Avena, S. Fiol, R. López, F. Arce, Effects of pH and ionic strength on the adsorption of phosphate and arsenate at the goethite-water interface, Journal of Colloid and Interface Science, 285 (2005) 476-486.
[41] S. Wang, X. Jin, Q. Bu, X. Zhou, F. Wu, Effects of particle size, organic matter and ionic strength on the phosphate sorption in different trophic lake sediments, Journal of Hazardous Materials, 128 (2006) 95-105.
[42] A. El Nemr, A. Khaled, O. Abdelwahab, A. El-Sikaily, Treatment of wastewater containing toxic chromium using new activated carbon developed from date palm seed, Journal of Hazardous Materials, 152 (2008) 263-275.
[43] B.H. Hameed, J.M. Salman, A.L. Ahmad, Adsorption isotherm and kinetic modeling of 2,4-D pesticide on activated carbon derived from date stones, Journal of Hazardous Materials, 163 (2009) 121-126.
[44] A.B. Albadarin, A.a.H. Al-Muhtaseb, N.A. Al-laqtah, G.M. Walker, S.J. Allen, M.N.M. Ahmad, Biosorption of toxic chromium from aqueous phase by lignin: mechanism, effect of other metal ions and salts, Chemical Engineering Journal, 169 (2011) 20-30.
[45] A.B. Albadarin, A.H. Al-Muhtaseb, G.M. Walker, S.J. Allen, M.N.M. Ahmad, Retention of toxic chromium from aqueous phase by H3PO4-activated lignin: Effect of salts and desorption studies, Desalination, 274 (2011) 64-73.
[46] T. Karthikeyan, S. Rajgopal, L.R. Miranda, Chromium(VI) adsorption from aqueous solution by Hevea Brasilinesis sawdust activated carbon, Journal of Hazardous Materials, 124 (2005) 192-199.
[47] M. Özacar, I.A. Sengil, A kinetic study of metal complex dye sorption onto pine sawdust, Process Biochemistry, 40 (2005) 565-572.
[48] Laleh Seifi, Ali Torabian, Hossein Kazemian, Golamreza Nabi Bidhendi, Ali Akbar Azimi, Farshid Farhadi, S. Nazmara, Kinetic Study of BTEX Removal Using Granulated Surfactant-Modified Natural Zeolites Nanoparticles, Water, Air, & Soil Pollution, 219 (2011) 443-457
[49] R.-L. Tseng, Mesopore control of high surface area NaOH-activated carbon, Journal of Colloid and Interface Science, 303 (2006) 494-502.
[50] Feng-ChinWua, Ru-Ling Tsengb, R.-S. Juang, Characteristics of Elovich equation used for the analysis of adsorption kinetics in dye-chitosan systems, Chemical Engineering Journal 150 (2009) 366–373.

464

465

466

467 **Figures**

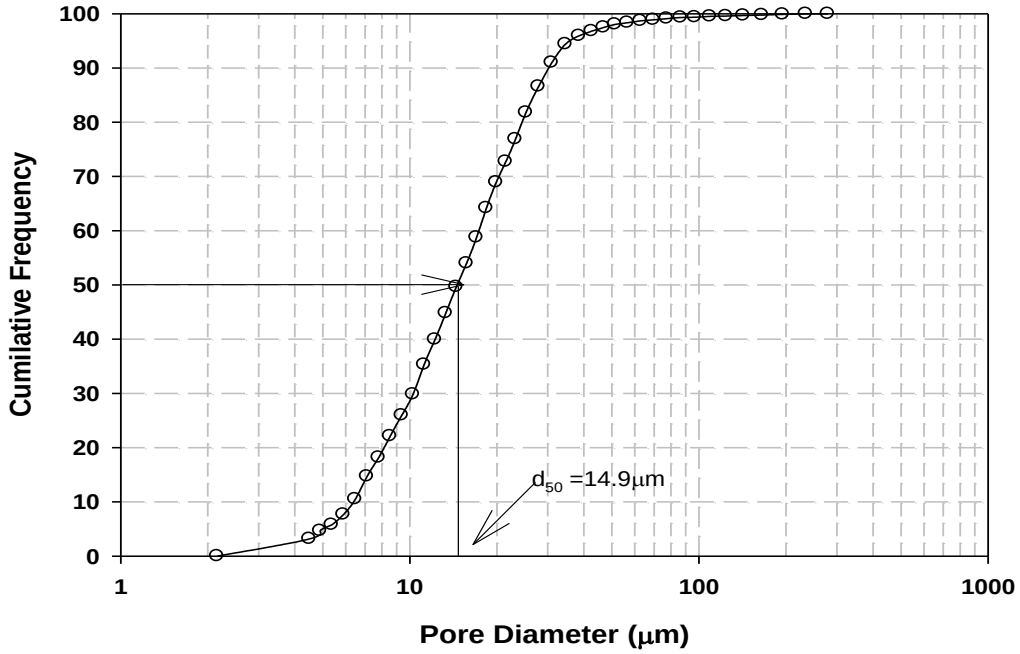

468

469 Fig. 1 : Cumulative pore size distribution curves of Fine Dolomite based on surface area.

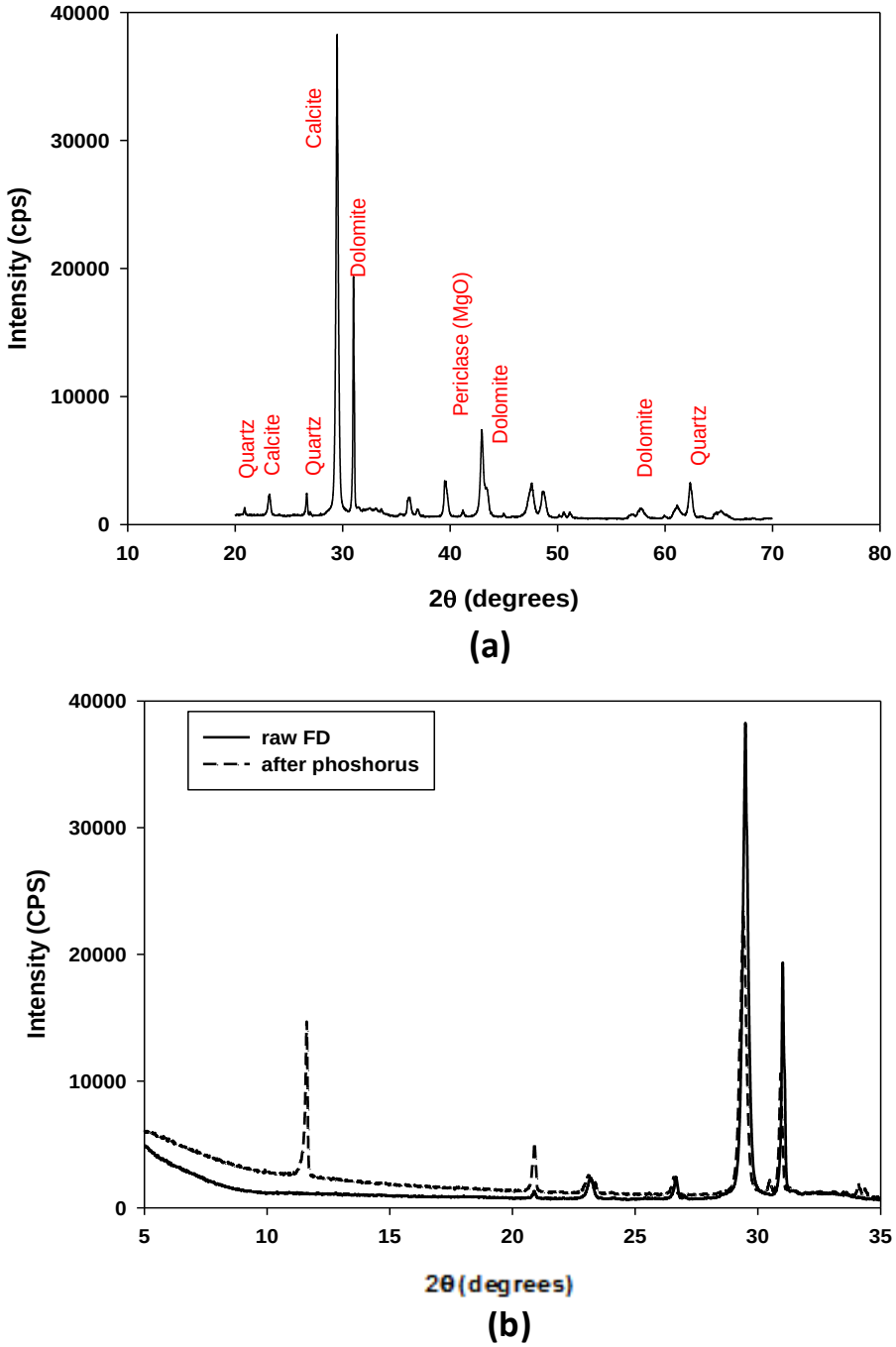

Fig. 2: XRD profiles of Fine Dolomite before (a) and after (b) adsorption of phosphate.

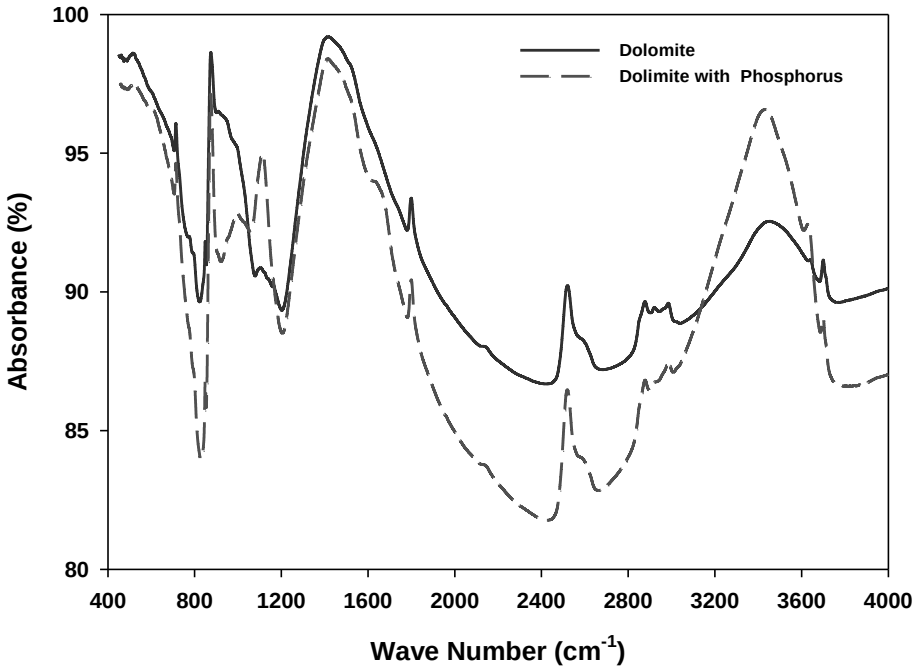

Fig. 3: FTIR spectrum of dolomite before and after phosphate adsorption.

485 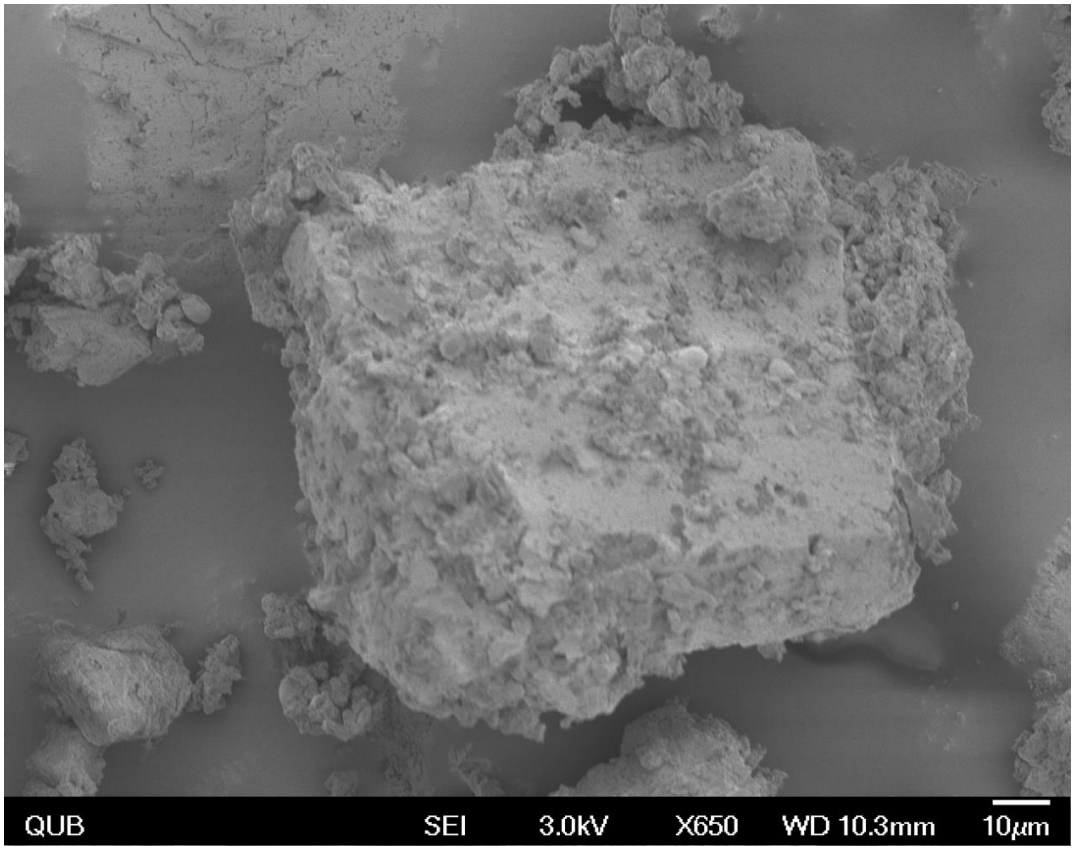

486 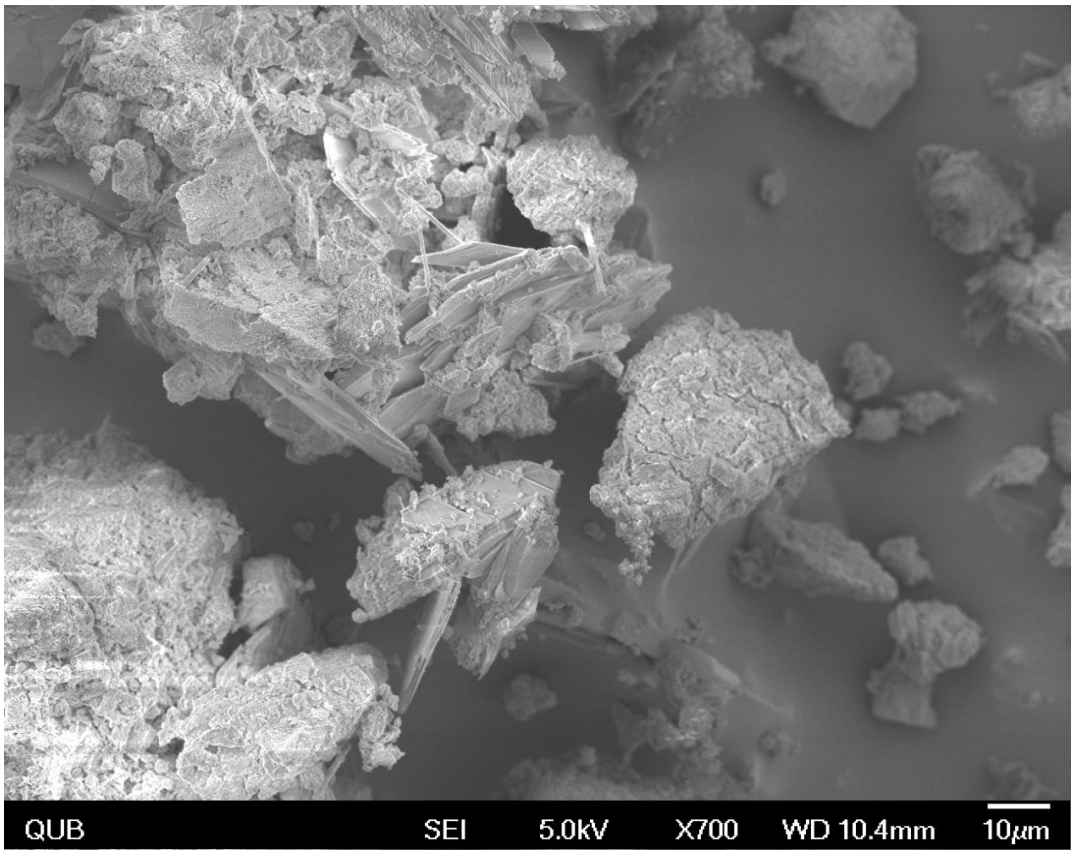

487 Fig. 4: The SEM micrographs of dolomite before and after phosphate adsorption.

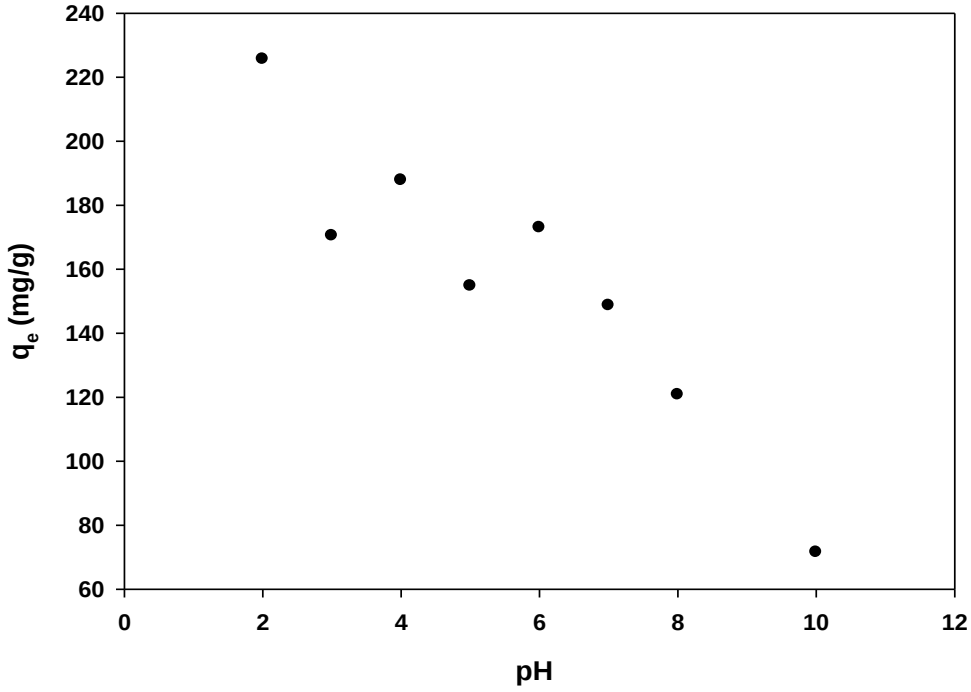

Fig. 5: Effect of pH solution on the adsorption of phosphate ions onto fine dolomite adsorbent.

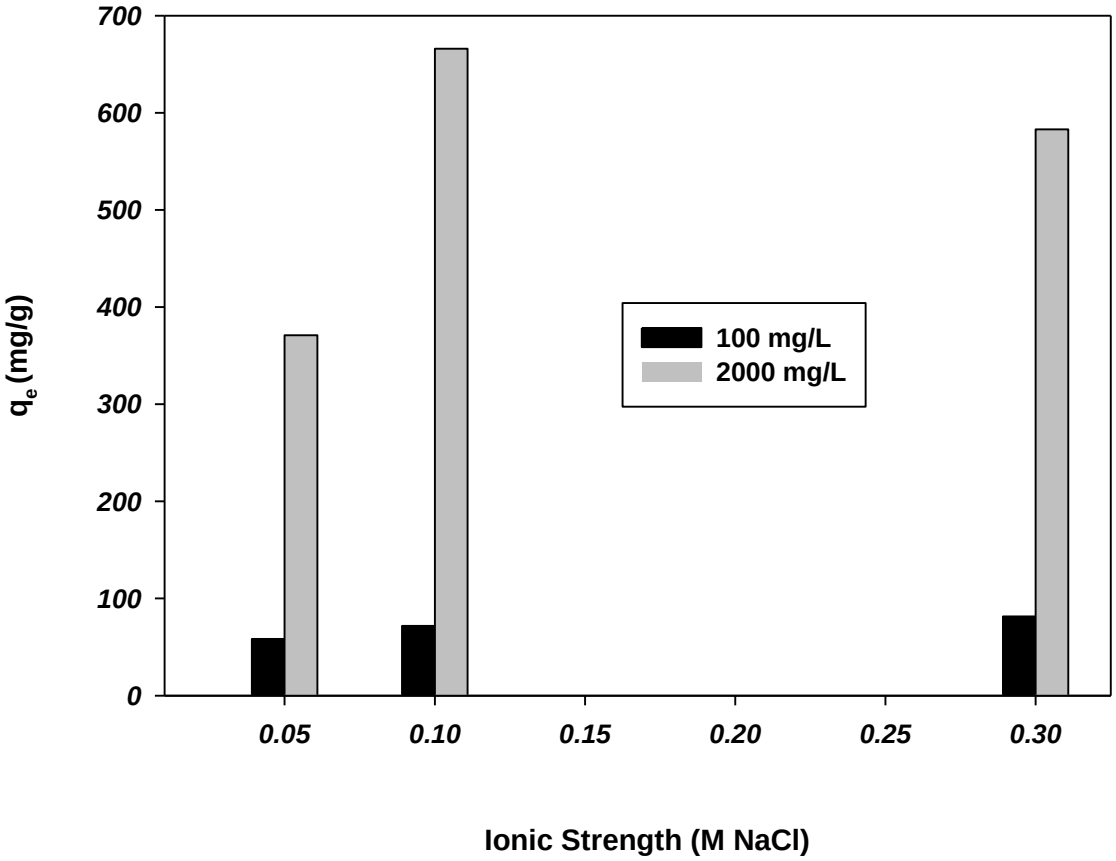

Fig. 6: Effect of ionic strength on adsorption of phosphate on fine dolomite.

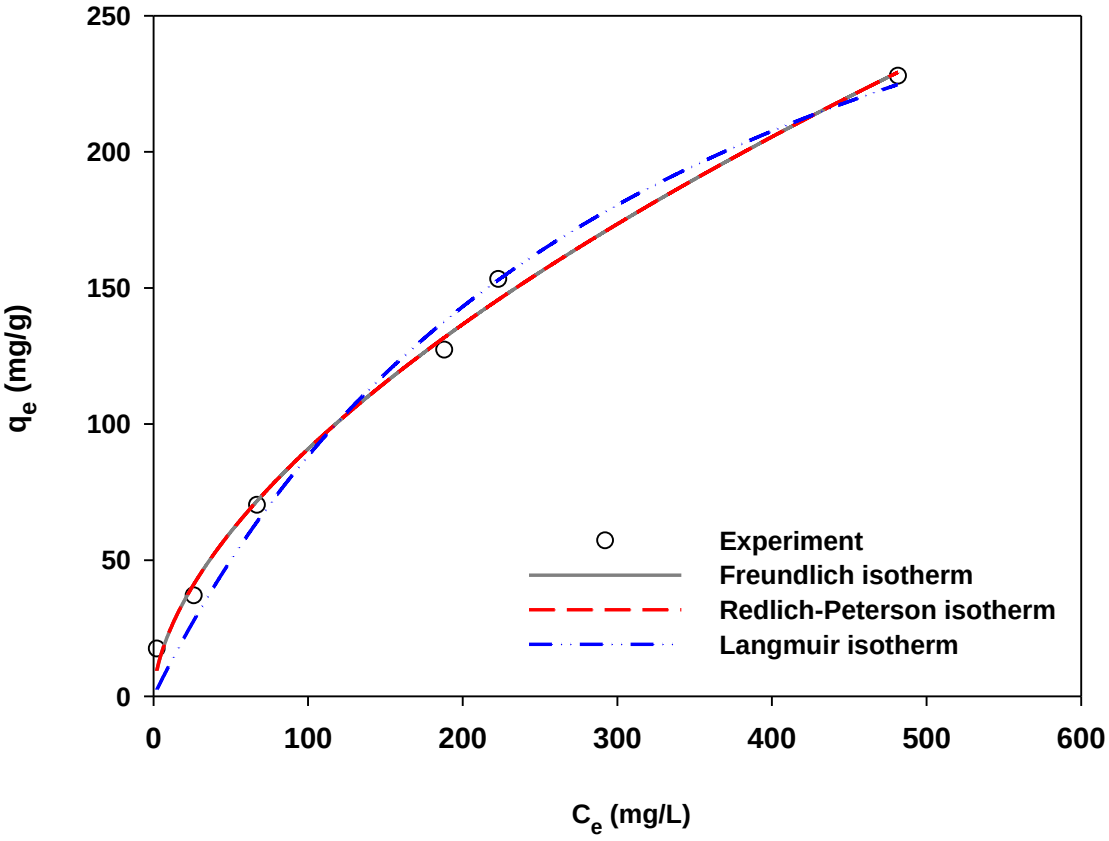

504

505 Fig. 7: Non-regression fits of Freundlich, Langmuir, Temkin and Redlich & Peterson models to the

506 adsorption equilibrium data.

507

508

509

510

511

512

513

514

515

516

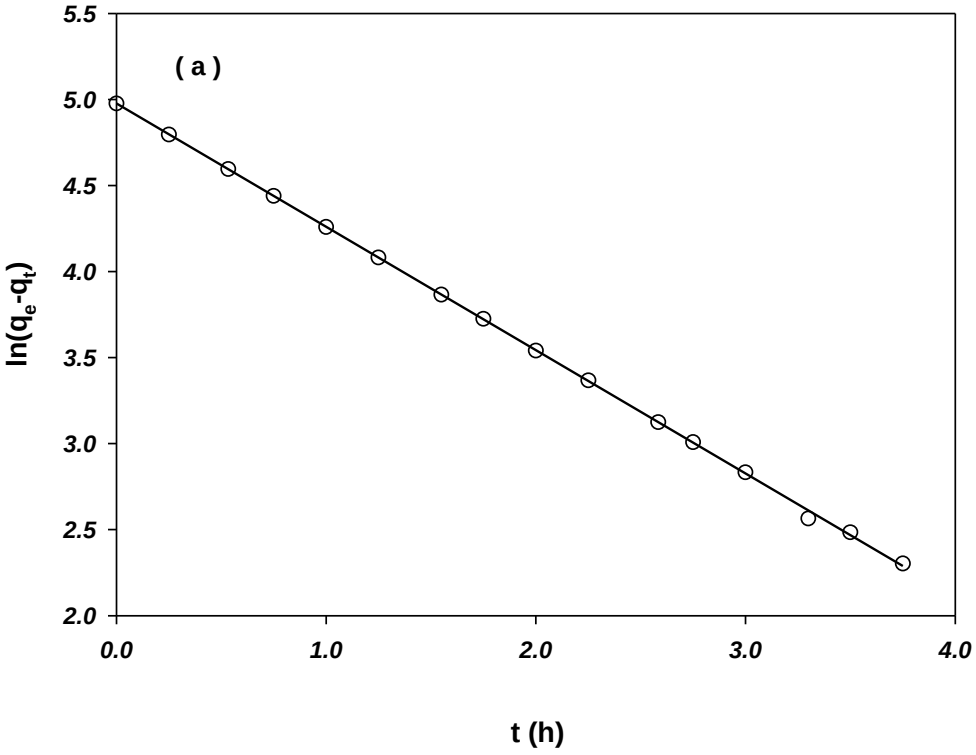
(a)
5.5
5.0
4.5
4.0
3.5
3.0
2.5
2.0
ln(qe-qt)
0.0
1.0
2.0
3.0
4.0
t (h)

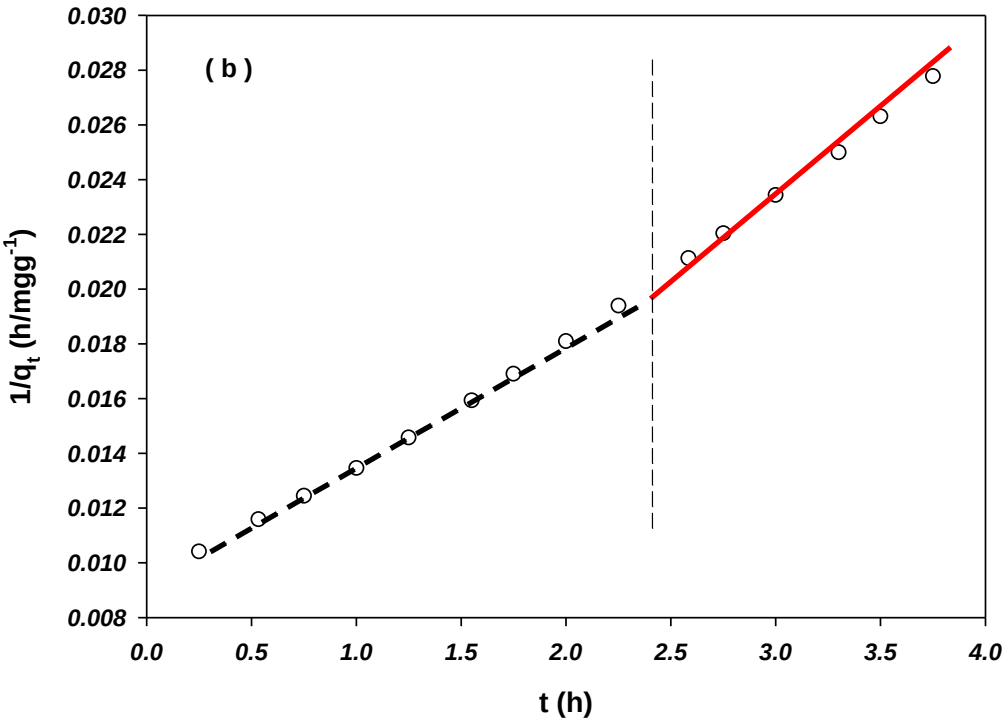
(b)
0.030
0.028
0.026
0.024
0.022
0.020
0.018
0.016
0.014
0.012
0.010
0.008
1/qt (h/mgg-1)
0.0
0.5
1.0
1.5
2.0
2.5
3.0
3.5
4.0
t (h)

517

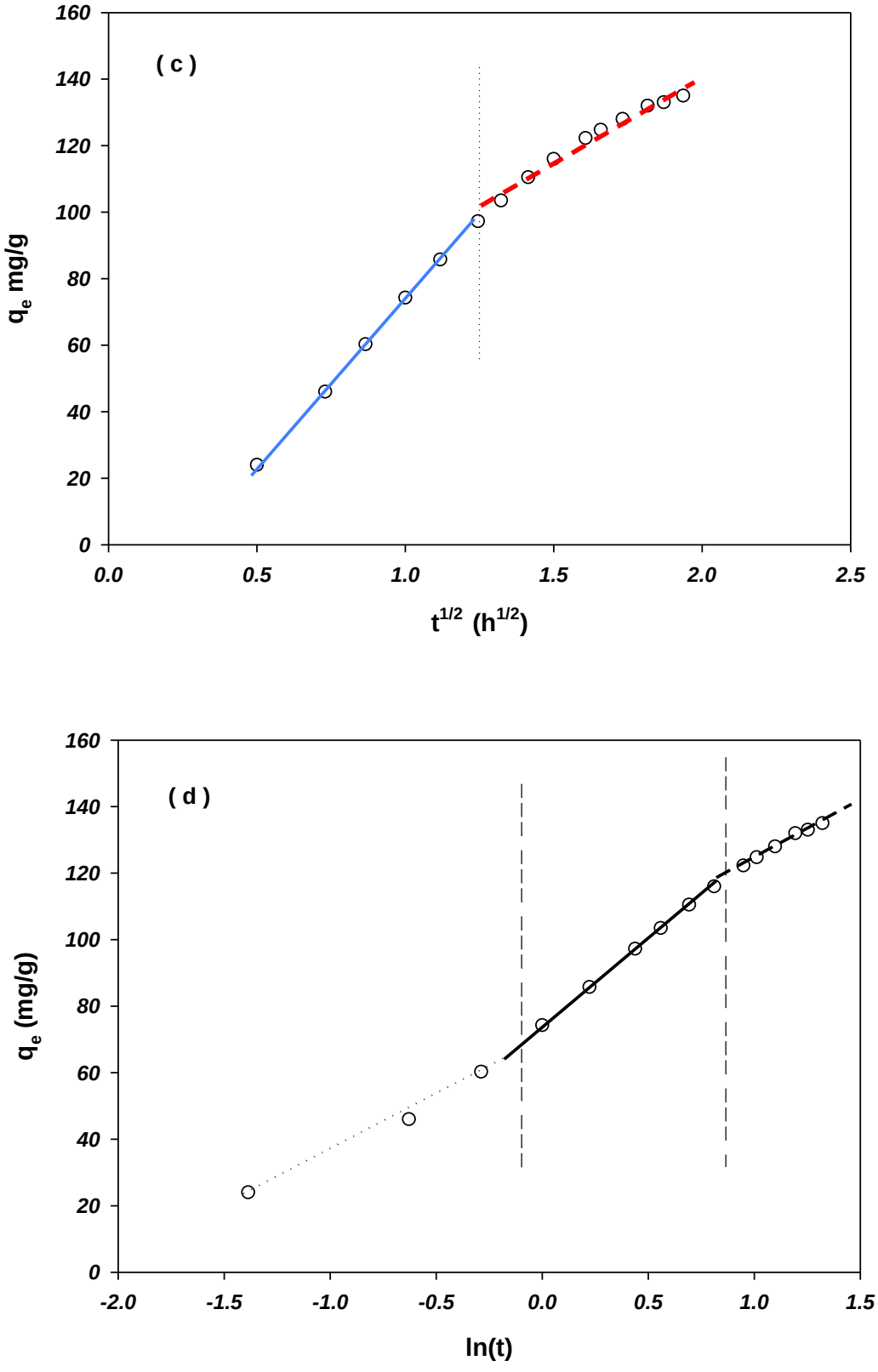

518

519 Fig. 8: Linearized plots of the different kinetic isotherms (a) Pseudo-first-Order (b) Pseudo-second-

520 order Model (c) Intra-particle diffusion (d) Elovich equation.

Tables

Table 1: Quantitative composition of the fine Dolomite powder.

No.	Compound Name	Chemical Formula	SemiQuant (%)
1	Calcium Carbonate	$CaCO_3$	68
2	Quartz	SiO_2	9
3	Dolomite	$CaMg(CO_3)_2$	14
4	Periclase	MgO	9

Table 2: Summary of model parameters form non-linear regress fits of different isotherms to experimental data obtained at different ionic strength.

Isotherm	Parameter	NaCl Concentration			
		0.0 M	**0.05 M**	**0.10 M**	**0.30 M**
Freundlich	K_F	6.029	63.40	21.20	34.85
	n	1.698	3.432	2.015	2.420
	SD	0.216	1.450	0.870	1.480
	R^2	0.995	0.609	0.887	0.785
Langmuir	q_{max}	377.8	616.8	984.9	851.0
	a_L	0.003	0.005	0.0023	0.003
	R_L	0.143	0.088	0.173	0.134
	SD	0.405	0.990	0.670	1.380
	R^2	0.985	0.759	0.938	0.587
Redlich–Peterson	K_R	1.47×10^7	1.651	1.287	1.391
	$a_R \times 10^{10}$	2.440	1.180	1.170	1.130
	β	0.411	0.271	0.323	0.326
	SD	0.344	0.450	0.380	1.000
	R^2	0.995	0.983	0.991	0.957

Table 3: Summary of the model parameters for the Kinetic models fitted to the kinetic data for adsorption of phosphate on fine dolomite.

Model	Parameter	
Pseudo-first-order	k_1 (h^{-1})	0.716
	q_e (mg P $g^{-1)}$	145.0
	SD	0.003
	R^2	0.999
Pseudo-second-order	k_2 (gm $g^{-1}h^{-1}$)	0.003
	q_e (mg g^{-1})	198.7
	SD	0.024
	R^2	0.999
Intra particle diffusion	K_{di} (mg $g^{-1}h^{-0.5}$)	73.84
	C_i (mg g^{-1})	1.25×10^{-11}
	SD	0.156
	R^2	0.999
Elovich model	a	258.1
	b	0.022
	SD	0.089
	R^2	0.996

548

549

550 Table 4: Comparison of adsorption capacities of the adsorbents.

Adsorbent	Adsorption capacity	pH	Max Conc. (mg/L)	Fit isotherm	Reference
Fine dolomite	377.8 (mg P/g)	2	2000	Redlich–Peterson	Current study
Iron-loaded tannin gel	31.3 (mg/g)	–	200	Freundlich	[1]
Alunite	4.69 (mol/g)	5	–	Langmuir	[15]
Mesoporous ZrO_2	29.7 (mg/g)	2–3	300	Langmuir	[30]
Fe–Mn binary oxide	36.0 (mg/g)	3	40.0	Freundlich/ Langmuir	[32]
Peat	8.91 (mg/g)	6.5	–	Langmuir	[35]

551

552